Integration and Interpretation of Aeromagnetic, 3D Seismic and Well Logs Data in Hydrocarbon Exploration in Niger Delta Basin

**Oluwatoyin O. Akinsete[1*], Toyin Y. Abdulraheem[1], Salawu B. Naheem[2]
and Adebiyi S. Leke[3]**

[1]*Department of Petroleum Engineering, University of Ibadan, Ibadan, Nigeria.*
[2]*BS Geophysical and Consultancy Ltd., Ilorin, Nigeria.*
[3]*Department of Physical Sciences, Landmark University, Omu-Aran, Nigeria.*

Authors' contributions

Article Information

Original Research Article

ABSTRACT

As the challenges associated with hydrocarbon exploration rises with upsurge in energy demand, the need to minimize risk associated with hydrocarbon exploration if supply is to keep up with demand.
In this work, high resolution aeromagnetic, 3D seismic and well-logs data were adopted and integrated to aid in exploration and characterization of reservoirs in "XYZ" field in offshore Niger Delta. Fast Fourier Transform Filter using Oasis Montaj software was applied to the Total Magnetic Intensity grid in horizon and fault interpretation also used to produce subsurface structural maps for sedimentary layer thickness estimation. Direct hydrocarbon indicators (bright spots) on the seismic section was shown using seismic signal. Petrel software and wireline log signatures were used to

_____

Corresponding author: E-mail: oo.akinsete@ui.edu.ng, oo.akinsete@mail1.ui.edu.ng;

identify hydrocarbon-bearing sands and determine petrophysical parameters such as porosity, hydrocarbon saturation and net thickness.

The structural maps generated showed: Three major (synthetic) faults dips south and one minor (antithetic) fault dips north in the field; three identified prospective sands (A, B, C) were delineated. Possible presence of oil accumulation was indicated by the combined Neutron-Density log response. The range of values of effective porosity, hydrocarbon saturation and net thickness were 18-22%, 34-58% and 19.1-28.1 m, respectively.

This study established that integration of magnetic, 3D seismic and well-log data are desirable innovative techniques to better understand and analyze subsurface for hydrocarbon potential and exploration.

NOMENCLATURES

HCIIP   :Hydrocarbon initially in-place
A   :Area extent of accumulation
h   :Average thickness (or net pay) of the reservoir
ϕ :Average effective porosity
N/G :net-to-gross
S_w :Average water saturation
ρ_{ma} -Matrix density
ρ_f :Fluid density
ρ_b :Bulk density read from log
n   :Saturation exponent (usually near 2)
a   :Empirical constant (usually near unity)
m   :Cementation factor (usually near 2)
R_w :Resistivity of formation water, Ωm
R_t :Resistivity of uninvaded formation, Ωm
I_{GR} :Gamma-ray Index
$GR_{\log}$:Gamma-ray log of information of interest
$GR_{\min}$:Gamma-ray log reading in sand formation
$GR_{\max}$:Gamma-ray log reading in shale formation
R :Reflection coefficient
Z_1 :Acoustic impedance of layer above
Z_2 :Acoustic impedance of layer below

1. INTRODUCTION

Hydrocarbon resources have always been important and essential natural resources to the general economic development of different countries in the world. There is need to sustain the production of these resources, so as to maintain and improve the general standard of living within these countries. Owning to the fact that, there is high cost incurred in the exploration of these vital resources, therefore it is very important to achieve maximum perfection in its detection and analysis for its quantification. According to [1], since cost effectiveness is one of the major challenging factors in the oil and gas industry, hydrocarbon exploration, reservoir interpretation and analysis should be thoroughly subjected to the best available technology to achieve the lowest level of uncertainty in its exploration and production. Drilling of an oil well, to maximize optimum production can be very enormous and costly project to embark on, coupled with the fact that there is rapid depletion of hydrocarbon reserves. Hence, it is imperative to exploit new development with innovative techniques. Therefore, the integration and interpretation of magnetic, seismic and well logs data provides a better concept for exploration and exploitation of hydrocarbon potential. Within a selected area, magnetic information complements seismic and well logs data in the interpretation of basin basement structures and understanding of geological features.

Aeromagnetic survey technique is a notable geophysical method which has been used effectively to investigate subsurface geology in different capacity such as archeological, geothermal, hydrocarbon and mineral studies. Studies of aeromagnetic data with interest in hydrocarbon exploration have been performed in recent years [2,3]. The study that employed aeromagnetic data of Muglad Basin in South Sudan discovered magnetic anomalies which clustered along a prospective structure and coincided with the Jarayan oil field [2]. A major advantage of aeromagnetic survey is the accessibility to cover major inaccessible areas that might prove expensive and slower to map out. For hydrocarbon resources, the aeromagnetic surveys are used at the initial

stages to map out and evaluate the thickness of the sedimentary basin [4]. This is achievable by analyzing and estimating the depths of the magnetic sources (i.e. the magnetic basement rocks causing the observed anomalies) within the study area. Largely, this is subjected to the fact that sedimentary rocks are non-magnetic for all intents and purposes [5]. Therefore, any magnetic variations observable at the surface are more likely to be associated with the magnetic sources from basement rocks. Nevertheless, exceptions to this assumption are some iron deposit, volcanic sequence, dykes and sills that are concealed within the surface sedimentary basin. In other to obtain qualitative interpretation by proper visualization of the subsurface geological structures, the data acquired from the aeromagnetic surveys are generally presented in gridded magnetic maps [4,5].

Seismic data can be said to be the most widely used tool in hydrocarbon reservoirs exploration and production. Basically, it helps in proper understanding and interpretation of the subsurface geometry, structures and potential hydrocarbon trappings [6-10]. Seismic application involves the movement of signal through the subsurface, by generation and propagation of seismic waves. These generated waves are sent down into the Earth's formation (subsurface) until they encounter discontinuity (boundaries) and are reflected back to the surface. Hence, these waves are recorded and carefully interpreted for possible hydrocarbon trapping within the subsurface [11,12]. In other to better understand the subsurface, so as to determine some important reservoir petrophysical properties (i.e. water saturation, porosity, permeability, volume of shale, hydrocarbon saturation, etc.) and estimate the hydrocarbon volume within the reservoir, several vertical measured wireline logs against reservoir depth, such as gamma ray, resistivity log, sonic log, neutron log, etc., can be employed to determine various reservoir physical properties of rock units [11]. Analysis and integration of seismic data together with well logs data can effectively improve the accuracy of reservoir characterization [10,13-16].

Hence, the required minimal level of uncertainty needed in hydrocarbon exploration and interpretation, gave rise to multidimensional approach of combining geophysics, geology, petrophysics, reservoir engineering and geostatistics for detailed reservoir evaluation [17]. Therefore, in this present work magnetic data, 3D seismic data and a suite of borehole geophysical well logs are utilized to reveal the potential of combining these three methods for the exploration and interpretation of the hydrocarbon potential of an oil field in offshore, Niger Delta with the objectives to: establish the effectiveness of using magnetic data, seismic data and well log data in hydrocarbon exploration, reservoir characterization; generate structural maps of the identified reservoir top; delineate type of hydrocarbon traps from the generated structural maps.

1.1 Location and Geological Setting

The field under consideration, identified as "XYZ" for the purpose of this study, is an offshore oil field located in the Niger Delta region, southern part of Nigeria. The field is situated in the western part offshore Niger Delta located between latitude 4° 37' 11.78" N - 4° 37' 15.48" N and longitude 6° 45' 39.23" E - 6° 50' 36.89" E. Niger Delta is situated on the Gulf of Guinea in the southern part of Nigeria (Fig. 1), it covers an area between latitude 3^oN and 6^oN and Longitude 4^oE and 8^oE. The Niger Delta basin is bounded to east and west by the Calabar Flank and Benin Flank respectively, the Gulf of Guinea to the south and in the north by older (Cretaceous) tectonic structures like Anambra Basin, Abakiliki uplift and Afikpo Syncline. It has a thickness of more than 10km that is composed of overall regressive clastic sequence, and a delta which prograde southwestward to form major active depobelts. The Niger Delta is rated amongst the productive hydrocarbon tertiary deltas in the world and covers an area of 75,000 km^2 [18,19].

The Niger Delta province, which is predominantly a sedimentary basin, has been identified to consist of three broad major formations (Akata, Agbada and the Benin formations) that extends southwards deep into the ocean. The petroleum system in Niger Delta is referred to as the Tertiary Niger Delta (Akata-Agbada) Petroleum System. The Akata formation which is the lower part, consist of predominant under compacted, over pressured thick shales, clays and siltstones sequences with some turbidities sandstones, while the Agbada formation which is made up of intercalation of paralic sandstones and shales is the transition zone, that represents the hydrocarbon (i.e. oil and gas) reservoir of the delta. It graded upward into massive continental sandstones to form an overlain, thereby forming the uppermost formation as the Benin formation [1,20].
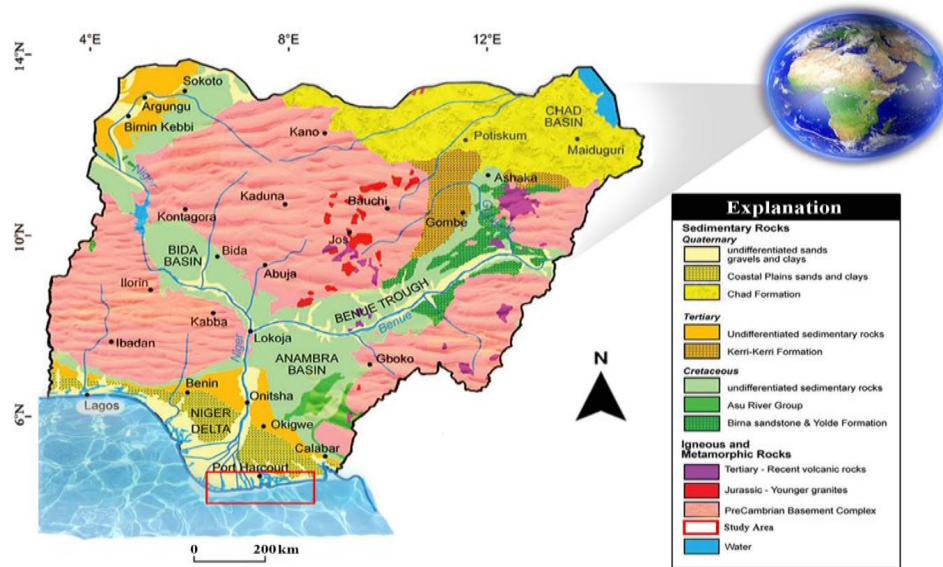
Fig. 1. The geologic map of Nigeria showing the Niger Delta and location of the study area
(Source: Salawu et al. 2019)

2. MATERIALS AND METHODS

The materials used for this study includes; Total magnetic intensity (TMI) anomaly map sheet numbered 329 (Fig. 2a) was acquired from the Nigerian Geological Survey Agency (NGSA), Oasis Montaj software package. 3D stacked depth migrated seismic sections comprising of 400 in-lines and 220 crosslines with a coverage area of about 52.96 km^2, base map of the study area (Fig. 2b), check shot survey curve and six spatially distributed well data, which comprises of composite logs suites including gamma ray, resistivity, sonic, neutron, and density logs, Schlumberger's Petrel software.

The survey was carried out along a sequence of NW–SE flight lines with a spacing interval of 500 m, an altitude of 80 m and tie lines of nearly 2 km interval. The International Geomagnetic Reference Field (IGRF) was used by NGSA to remove the Regional field. In order to estimate the thickness of the sedimentary layer which is essential in hydrocarbon exploration, the two dimensional power spectrum plot (Fig. 3) was applied to the TMI grid, this filter was applied using the commercially available Oasis Montaj software package. We applied power spectrum to the aeromagnetic data of the study area, in other to estimate average depths to shallow and deep magnetic sources [21].

Interpretation of seismic sections and well log data was done interactively in Petrel software, with well to seismic tie, from where three (3) sand units were mapped and evaluated by generating various indicator maps such as time and depth structural maps. The information is useful in determining appropriate locations for drilling exploratory, appraisal or development wells within a prospect. The well logs which have different records of physical borehole parameters taken against depth were duly interpreted for various petrophysical analysis and also utilized to carry out litho-stratigraphic correlation across the wells (Fig. 4), basically to help in the establishment of distribution and behavior of the lithological units of interest across different well locations. They were also employed for easy identification of porous and permeable lithological units with saturated hydrocarbon, which gives them the unique qualities that separates them as hydrocarbon reservoirs. In addition, the well log dataset was used to derive reservoir parameters such as, reservoir thickness, Net-to-Gross (NTG), volume of shale (Vsh) in the clastic reservoirs, effective porosity ($\varnothing_{eff}$), hydrocarbon saturation (S_h), which aids in the evaluation of hydrocarbon potential of field using equations (1-6).

$$HCIIP = A \times h \times \phi_{eff} \times N/G \times \left(1 - S_w\right) \qquad (1)$$

Where:

ϕ the total porosity is given as:

$$\phi = \frac{\rho_{ma} - \rho_b}{\rho_{ma} - \rho_f} \tag{2}$$

Effective porosity obtained from equation (3)

$$\phi_{eff} = \phi \times (1 - V_{sh}) \tag{3}$$

Volume of shale V_{sh} is given as:

$$V_{sh} = 0.083 \left(2^{3.7 \times (I_{GR})} - 1 \right) \tag{4}$$

$$I_{GR} = \frac{GR_{log} - GR_{min}}{GR_{max} - GR_{min}} \tag{5}$$

$$S_w = \sqrt[n]{\frac{a}{\phi^m} \frac{R_w}{R_t}} \tag{6}$$

In line with the aim of this work, the 3D seismic reflection data which consist of both in-lines and cross-line seismic sections were analyzed for horizon mapping, structural interpretation and attribute extraction, used to generate horizon surfaces, structural frameworks, time and depth structural maps. Relating the analyzed well data to seismic data (and vice versa) handled in vertical scale units. Well-to-seismic ties allow well data measured in units of depth to be compared to seismic data measured in units of time by convolving the generated reflectivity series derived from Zeoppritz reflectivity equation (7) with a zero phase wavelet. This was done with the aid of generated synthetic seismogram (Fig. 5 and 6), which permits the basis for the
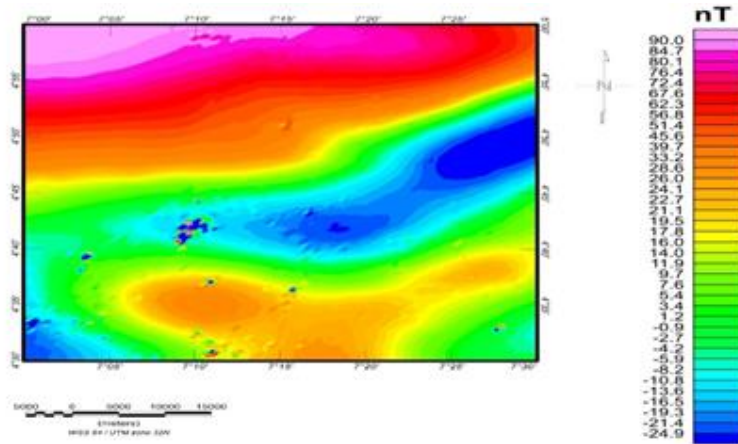

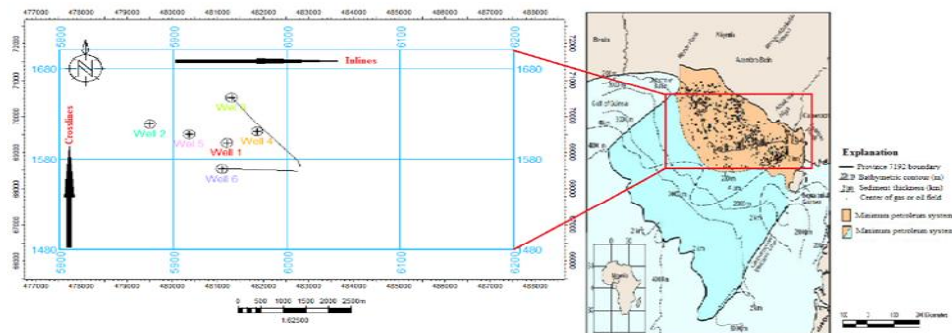**Fig. 2(a). Total Magnetic Intensity (TMI) anomaly map of the study area**

Fig. 2. (b). Base map of the study area showing the spatial distribution of wells within the seismic grid
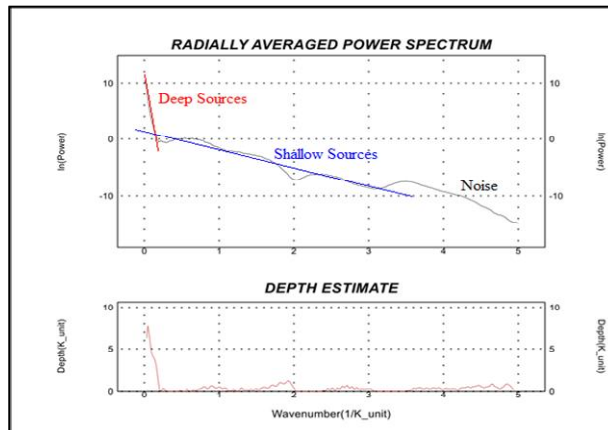
Fig. 3. Averaged power spectrum plot of the aeromagnetic data of the study area

horizon mapping and interpretation across the seismic cube. Mapping of seismic volume horizons involves the continuous outward tracing of the picked horizon across the seismic cube (at every 10th in-line and cross-line sections) from the seed points using the guided auto-tracking, 2D or 3D seeded auto-tracking tool provided by Petrel interpretation software (Fig. 7).

$$R = \frac{Z_2 - Z_1}{Z_2 + Z_1} \tag{7}$$

Three horizons were carefully traced out within the interpretation window and measured in seismic time (two-way time). Each was totally mapped across the in-line and cross-lines to generate horizon surface maps that indicate the spatial distribution of hydrocarbon formation within the subsurface. Time structural maps were generated for each of the mapped horizons, from

the derived horizon surface maps by making use of the fault polygons of delineated major faults. Afterwards, the time maps were converted to depth structural maps with the time-depth relationship by using the velocity function generated with the aid of sonic check-shot data. Both the time and depth maps were then compared for any inconsistency [10,22]. Finally, a series of surface and volume seismic attribute was run and extracted from the 3D seismic data provided using the Schlumberger's Petrel software. According to [19], extraction of seismic attributes from seismic data can bring to fore new information and insights into stratigraphic and structural interpretations. The deliverables from seismic attributes extraction and analysis will help greatly in reducing exploration and developmental risk, which helps us to better visualize or quantify features of interpretation interest.
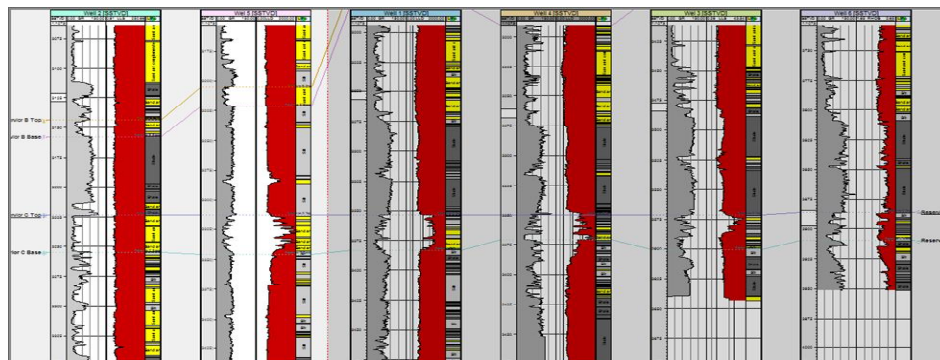

Fig. 4. Wells correlation panel showing lithological correlation from NW-SE showing sands A, B and C tops and bases, flatten on reservoir C top
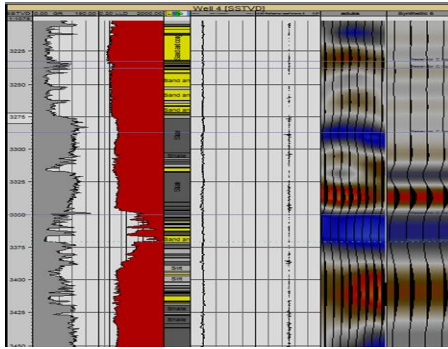
Fig. 5. Well to seismic tie section from well 4 showing panel tracks of gamma ray log, resistivity log, lithology log, acoustic impedance (AI), reflection coefficient (RC), seismic volume of "XYZ" field and the synthetic generated
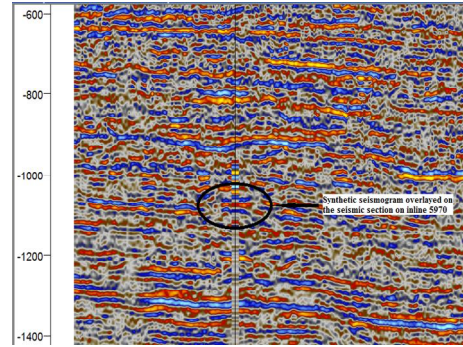

Fig. 6. Overlay of synthetic seismogram generated, within the seismic section on inline 5970
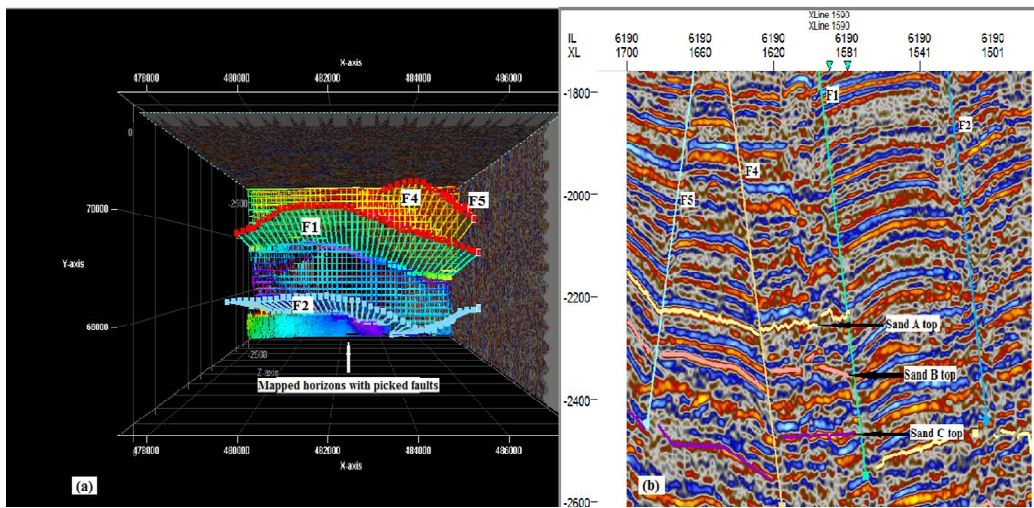

Fig. 7. Comparison of mapped horizons and faults of the study area (a) top view 3D seismic section of the mapped horizons and delineated faults (b) 2D seismic section of the horizons sand tops and delineated faults

3. RESULTS AND DISCUSSION

3.1 Magnetic Data Interpretation

The Total Aeromagnetic Intensity (TMI) anomaly map (Fig. 2a) showed negative and positive magnetic amplitude values between -24.9 nT and 90.0 nT. The studied area is located at non-polar and non-equatorial region; therefore, magnetic sources would be characterized by low magnetic anomalies instead of high magnetic anomalies. Although, the TMI anomaly map is generally occupied with E-trending positive anomalies, the central-eastern portion of the map reveals low

negative anomalies with amplitude values -24.9 to -0.9 nT. This is possibly due basement uplifts or intrusive structural features under the sediments with Niger Delta Basin.

The depth to magnetic basement information which can be utilized as proxy for overburden thickness of the region under study, are acquired from the estimated radial averaged power spectrum of the total aeromagnetic anomaly data. The power spectrum plot (Fig. 3) revealed essentially three components: the regional, residual and the noise signals. While the depth estimate chart (Fig. 3) provides estimated

average depths information of the regional and residual sources within the region. From the depth chart, top of regional sources is approximately 7 km and residual is approximately 0.5 km. Hence, the average thickness of the sedimentary pile within the region is highly favorable for hydrocarbon maturation, on condition that all other parameters for hydrocarbon accumulation are favorable, including average temperature gradient of 1^oC for 30m.

3.2 Seismic Interpretation

The generated synthetic seismogram (Figs. 5 and 6) used to identify the events that marks the top of sandstone and fault interpretations were carried out for subsurface structural interpretation. In all, three sands (A, B and C) were mapped on seismic sections over the entire field. The seismic cube indicated the presence of a total of five faults (Fig. 8a and 8b) - three major faults F1, F2 and F4 which are synthetic faults dipping basin ward that runs from the northwest to the southeastern (Fig. 8a), southern portion and the north eastern portion of the field respectively. They are structural building faults typical of the Niger Delta extensional zone. And two minor faults F3 and F5 are antithetic fault dipping landward located at the southwest part of the field (Fig. 8a and 8b). There are growth faults and these gives rise to fault assisted structure i.e. rollover anticline. The delineated faults were further confirmed with the Ant-Tracking volume attribute extracted on each of the reservoirs sand (Figs. 11, 14 and 17). The time and depth structural maps generated indicated the presence of a major closure in all the sands, all falling on the same position along the vertical axis in the center of the field. Although, more closures are visible, but not identified because they are outside the region of the drilled exploratory wells. The principal hydrocarbon entrapment in the field were identified and located at the center of the field which probably corresponded to the crest of the roll over structure observed on the seismic sections. This was observed as fault assisted closures on the time structure map of the sand (Fig. 9, 12 and 15). Maximum magnitude (surface) and Envelope (volume) attributes maps were used to confirm the presence and position of hydrocarbon accumulation in these sands.

3.3 Petrophysical Analysis

The petrophysical parameters obtained from the delineated reservoir sands (Fig. 4) are shown in

Table 1. It could be observed in sand A that the average effective porosity is 0.18. Water saturation of average value of 0.55 is fairly high while the average hydrocarbon saturation is 0.45, which is a good value for hydrocarbon accumulation. From Table 2, sand A has its maximum thickness at 85.73ft (26.13m) and minimum thickness at 49.54ft (15.10m), with an average of 72.10ft (21.97m) across the wells. In sand B, the average effective porosity is 0.22. Water saturation is high with an average value of 0.66 and the average hydrocarbon saturation is 0.34. The sand has its maximum thickness at 93.01ft (28.35m) and minimum at 45.08ft (13.74m), and an average of 62.57ft (19.07m) across the entire wells. For sand C, the average effective porosity was 0.19 while average hydrocarbon saturation was 0.58 and relatively moderate average water saturation of 0.42. In this sand, the maximum thickness is at 109.78ft (33.46m) and minimum at 69.09ft (21.06m) and an average of 92.32ft (28.14m) across the wells.

3.4 Interpretation for Sand A

The time structural map of sand A (Fig. 9a), structural highs are observed in the northeast and in the center of the field while structural lows are observed in the southwest. The depth structural map of Sand A (Fig. 9b) has its deepest part at a depth of 3288.91m (10790.39ft) whiles its shallowest depth at 2855.66m (9368.96ft). Using this information, it can be seen that the crest of the roll over structure (structural high), antithetic fault, F3 and growth fault, F1 act as good traps for the hydrocarbon accumulations in the sand at the center of the field. Most of the faults in the field served as support to the hydrocarbon trapping mechanism i.e. fault assisted closures and rollover anticlines. The maximum magnitude (surface) and envelope (volume) attributes (Figs. 10a and 10b) showed high amplitude anomaly i.e. direct hydrocarbon indicator (DHI) within the closure which gives strong evidence of presence of hydrocarbon within the sand. From the petrophysical analysis the reservoir has its maximum thickness of 26.13m (85.73ft) and minimum thickness of 15.10m (49.54ft) and an average of 21.97m (72.08ft) across the wells. Sand A is a probable prospect zone for hydrocarbon production as shown in the maximum magnitude attribute (Fig. 10a). The high amplitude anomaly (DHI) within the closure gives strong evidence of presence of hydrocarbon within the sand.

Table 1. Petrophysical result for the sands

Reservoir	Neutron-Density logs response	Hydrocarbon type	Average water saturation (S_w)	Average hydrocarbon saturation (S_h)	Average effective porosity ($\emptyset_{eff}$)	Average volume of shale (V_{sh})	Average net-to-gross (NTG)
Sand A	Intermediate neutron-low density	Oil	0.55	0.45	0.18	0.20	0.80
Sand B	Intermediate neutron-low density	Oil	0.66	0.34	0.22	0.23	0.77
Sand C	Intermediate neutron-low density	Oil	0.42	0.58	0.19	0.52	0.48

3.5 Interpretation for Sand B

Sand B has its deepest part at a depth of 3688.17m (12100.30ft) while its shallowest depth at 3143.80m (10314.30ft) according to the depth maps (Fig. 11b). Similar events occurred in these sands, from the time structural map of sand B (Fig. 11a), structural highs are observed in the northeast and in the center of the field while structural lows are observed in the southwest. Using this information, it can be seen that the crest of the roll over structure (structural high), antithetic fault, F3 and growth fault, F1 act as good traps for the hydrocarbon accumulations in the sand at the center of the field. Most of the faults in the field served as support to the hydrocarbon trapping mechanism i.e. fault assisted closures and rollover anticlines. The maximum magnitude (surface) and envelope (volume) attributes (Fig. 12a and 12b) shows high amplitude anomaly i.e. direct hydrocarbon indicator (DHI) within the closure which gives strong evidence of presence of hydrocarbon within the sand. Also, from the petrophysical analysis the reservoir has its maximum thickness of 28.35m (93.01ft) and minimum thickness of 13.74m (45.08ft) and an average of 19.07m (62.57ft) across the wells. Sand B is a probable prospect zone for hydrocarbon production as shown in the maximum magnitude (surface) attribute (Fig. 12a).

3.6 Interpretation for Sand C

Sand C has its deepest part at a depth of 3909.52m (12826.51ft) while its shallowest depth at 3223.32m (10575.20ft) according to the depth maps (Fig. 13b). Similar events occurred in these sands, from the time structural map of sand C (Fig. 13a), structural highs are observed in the northeast and in the center of the field while structural lows are observed in the southwest. Using this information, it can be seen that the crest of the roll over structure (structural high), antithetic fault, F3 and growth fault, F1 act as good traps for the hydrocarbon accumulations in the sand at the center of the field. Most of the faults in the field served as support to the hydrocarbon trapping mechanism i.e. fault assisted closures and rollover anticlines. The maximum magnitude (surface) and envelope (volume) attributes (Fig. 14a and 14b) showed high amplitude anomaly (DHI) within the closure which gives strong evidence of presence of hydrocarbon within the sand. From the petrophysical analysis, the reservoir has its maximum thickness of 33.46m (109.78ft) and minimum thickness of 21.06m (69.09ft) and an average of 28.14m (92.32ft) across the wells. Sand C is a probable prospect zone for hydrocarbon production as shown in the maximum magnitude (surface) attribute (Fig. 14a).
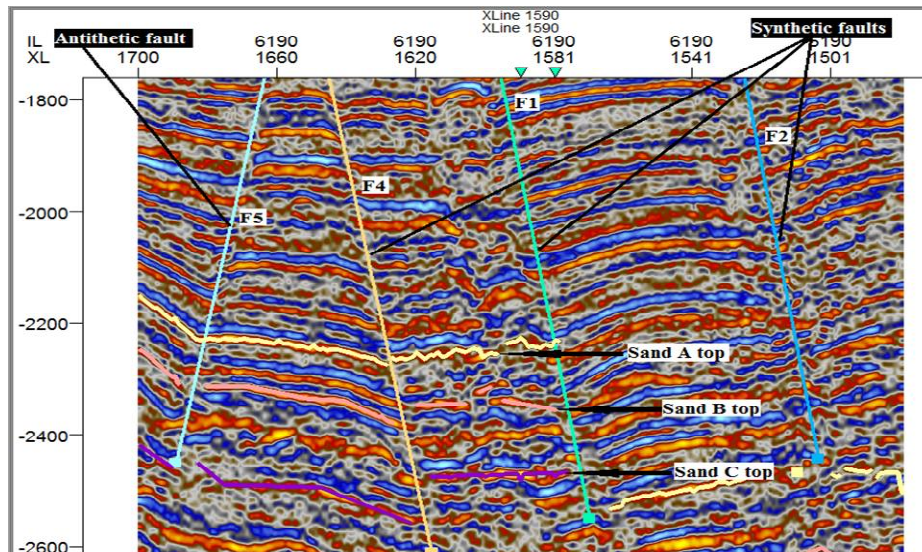

Fig. 8. (a) Typical 2D interpretation seismic section on inline 6190 showing picked horizons of sand tops and delineated synthetic and antithetic faults; F1, F2, F4 and F5
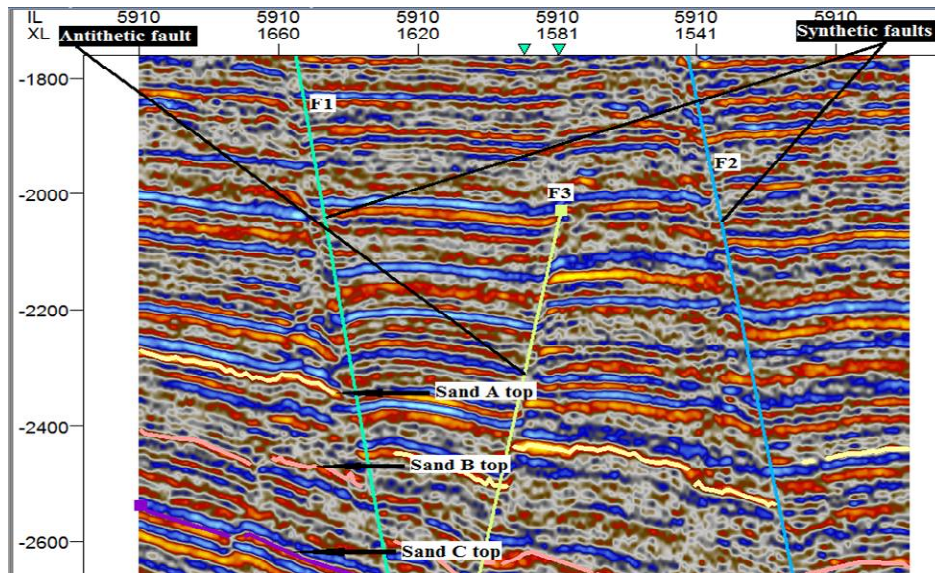
Fig. 8. (b) Typical 2D interpretation seismic section on inline 5910 showing picked horizons of sand tops and delineated synthetic and antithetic faults; F1, F2 and F3

Table 2. Stratigraphic thickness of the sand units against well

Well		Sand A (meters)	Thickness (meters)	Sand B (meters)	Thickness (meters)	Sand C (meters)	Thickness (meters)
Well 1	Top	2855.66	25.08	3161.56	14.62	3353.55	29.85
	Base	2880.74		3176.18		3383.40	
Well 2	Top	2863.12	22.69	3143.80	13.74	3223.32	31.66
	Base	2885.81		3157.54		3254.98	
Well 3	Top	2982.94	18.52	3360.00	28.35	3571.00	28.96
	Base	3001.46		3388.35		3599.96	
Well 4	Top	2873.60	15.10	3176.17	14.67	3349.86	21.06
	Base	2888.70		3190.84		3370.92	
Well 5	Top	2912.32	26.13	3205.80	15.56	3312.56	33.46
	Base	2938.45		3221.36		3346.02	
Well 6	Top	3264.64	24.27	3660.67	27.50	3885.68	23.84
	Base	3288.91		3688.17		3909.52	
Average Thickness			21.97		19.07		28.14
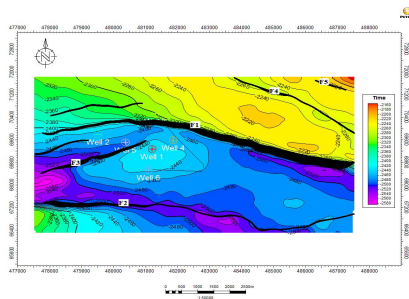
Fig. 9. (a) Time structural map of sand a with interpreted faults
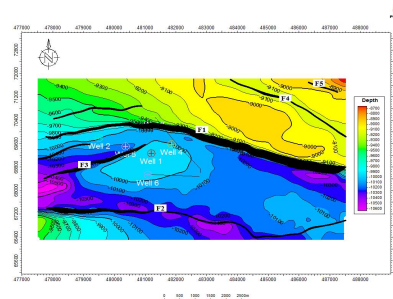
Fig. 9. (b) Depth structural map of sand a with interpreted faults
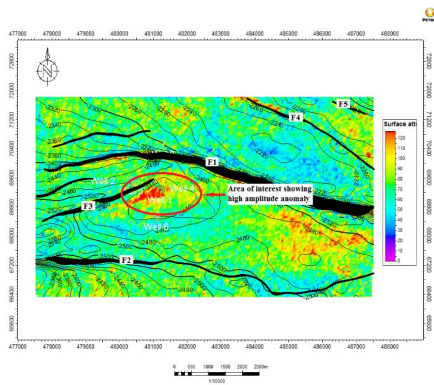
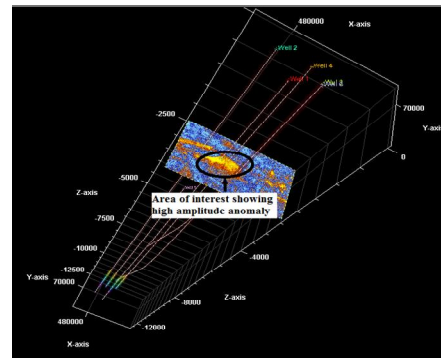**Fig. 10. (a) Maximum magnitude (surface) extracted on sand A**

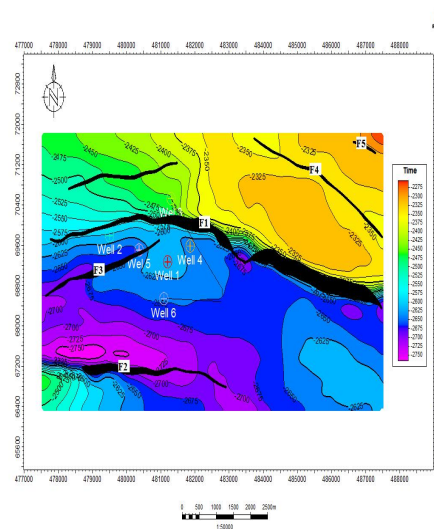**Fig. 10. (b) Envelope (volume) attributes extracted on sand A**

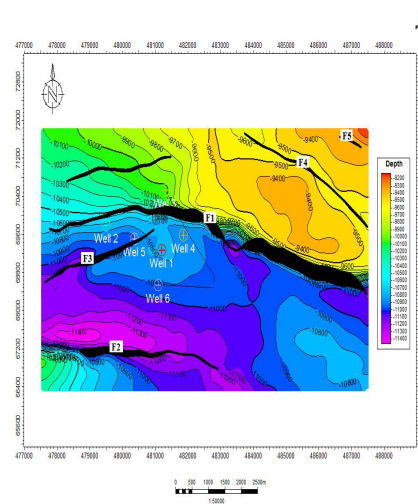**Fig. 11. (a) Time map of sand B with interpreted faults**

Fig. 11. (b) Depth structural map of sand B with interpreted faults
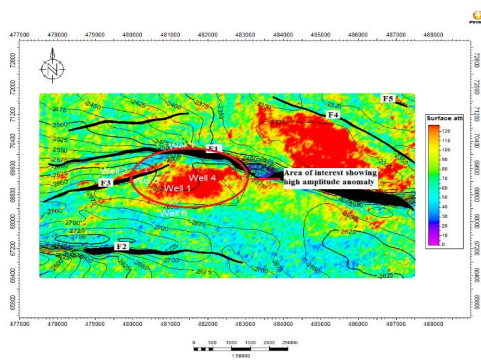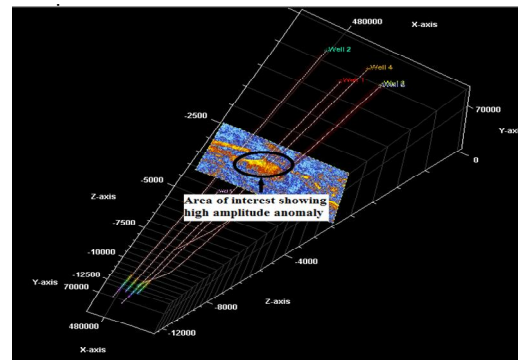

Fig. 12. (a) Maximum magnitude (surface) extraced on sand B

Fig. 12. (b) Envelope (volume) attributes extracted on sand B
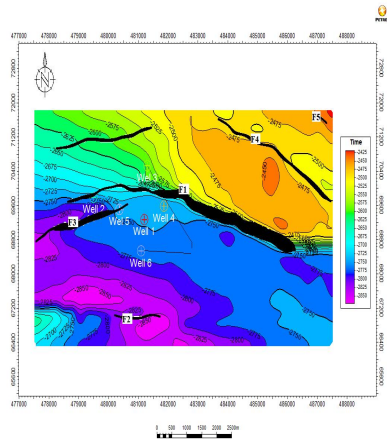
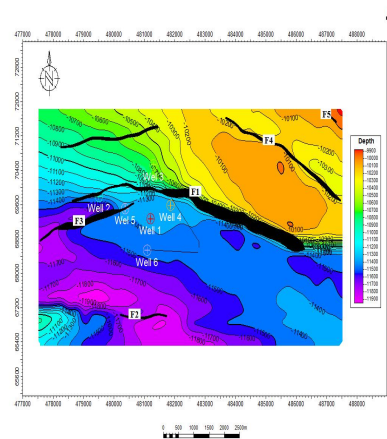**Fig. 13. (a) Time structural map of sand C with interpreted fault**

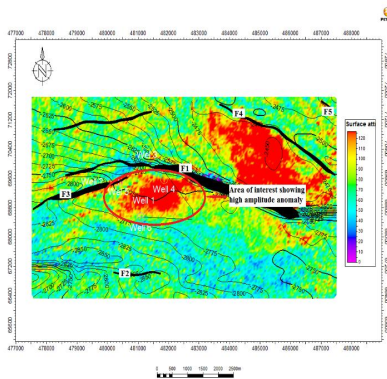**Fig. 13. (b) Depth tructural map of and C with interpretedfaults**

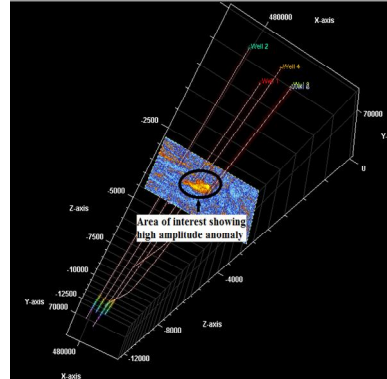**Fig. 14. (a) Maximum magnitude (surface) extraced on sand C**

Fig. 14. (b) Envelope (volume) attributes extraced on sand C

4. CONCLUSION

In this study, aeromagnetic data, seismic data and well logs data are effectively integrated as a viable and an innovative technique in hydrocarbon interpretation analysis which provides a better concept of understanding the subsurface for hydrocarbon potential and in accurate delineation of reservoir blocks in the study area. The two dimensional power spectrum plots were applied on the total aeromagnetic intensity (TMI) anomaly map of the area under study, which was able to give an average estimated depth thickness of the sedimentary pile within the region to be highly favorable for hydrocarbon maturation. Within the scope of this work, it was established that the trapping mechanisms in the field of study are fault assisted and rollover anticline. The petrophysical properties of 'XYZ" field also reflects the ability of the formation to store and produce hydrocarbon.

Three sandstone reservoirs prospects (sands A, B and C) were identified and interpreted to be hydrocarbon bearing sand and correlated across the field using 3-D seismic and well logs data in the Niger Delta basin. Subsequently, good tie was obtained for well-to-seismic data and structural traps were identified from the closures on the Time and Depth structural maps generated for the sand tops. The depth converted structural maps correlated with the time structural maps within the closure and various seismic signals attributes generated, which indicated large extent of bright spots (Direct Hydrocarbon Indicator) in the closure of sands A, B and C. The obtained results from this work will help shed more light into the structural framework of the study area and further assist greatly in delineation of hydrocarbon leads and prospects which subsequently help to reduce exploration and developmental risk, and also provide needful information that would guarantee

the best effective hydrocarbon production plan from the delineated reservoir compartments.

ACKNOWLEDGEMENTS

COMPETING INTERESTS

Authors have declared that no competing interests exist.

REFERENCES

1. Edigbue PI, Komolafe AA, Adesida AA, Itamuko OJ. Hydrocarbon reservoir characterization of "Keke" field, Niger Delta using 3D seismic and petrophysical data. American Journal of Scientific and Industrial Research. 2014;5(2):73-80.
2. Stones V, Fairhead JD, Oterdoom WH, Carigali P. The meter reader: Micromagnetic seep detection in the Sudan. The Leading Edge. 2004;23 (8):734-737.
3. Aderoju AB, Ojo SB, Adepelumi AA, Edino F. A Reassessment of hydrocarbon prospectivity of the Chad Basin, Nigeria, using Magnetic Hydrocarbon Indicators from High-Resolution Aeromagnetic Imaging. Ife Journal of Science. 2016;18 (2):503-520.
4. Salawu NB, Olatunji S, Adebiyi LS, Olasunkanmi NK, Dada SS. Edge detection and magnetic basement depth of Danko area, northwestern Nigeria, from low‑latitude aeromagnetic anomaly data. SN Applied Sciences. 2019;1:1056.
    Available:https://doi.org/10.1007/s42452-019-1090-3
5. Olowofela JA, Badmus BS, Ganiyu SA, Olurin OT, Babatunde P. Source location and depth estimation from digitized aeromagnetic data acquired from a basement complex formation. Earth Sci. India. 2011;4(3):136–142.
6. Ojo OA. Predrill Prospect Evaluation in Deepwater Nigeria. Nigerian Association of Petroleum Explorationists Bulletin. 1996;11:11-22
7. Balarabe HJ. Interpretation of Madu field 3D Seismic Data and Prospect Generation, A Paper delivered at a Technical Section to Exploration/Asset Department, Texaco Overseas Petroleum Company of Nigeria; 2003.
8. Adeoye TO, Enikanselu PA. Hydrocarbon reservoir mapping and volumetric analysis using seismic and borehole data over "Extreme" field, Southwestern Niger Delta. Ozean Journal of Applied Sciences. 2010; 2:4.
9. Bob H. Using seismic technologies in oil and gas exploration; 2013.
    Available:http://earthsky.org/earth/bob-hardage-using-seismic-technologies-in-oil-gsexploration.
10. Osinowo OO, Ayorinde JO, Nwankwo CP, Ekeng OM, Taiwo OB. Reservoir description and characterization of Eni field Offshore Niger Delta, southern Nigeria. Journal of Petroleum Exploration and Production Technology. 2017;8(2): 381-397.
11. Schlumberger. Log Interpretation, Principles and Application: Schlumberger Wireline and Testing, Houston, Texas. 1989;21-89.
12. Asquith N. Basic Well Log Analysis for Geologists. A.A.P.G Methods in Exploration. Tulsa, Oklahoma. 2004;16: 12–135.
13. Odoh BI, Onyeji J, Utom AU. The Integrated Seismic Reservoir Characterization (ISRC) study in Amboy Field of Niger Delta Oil Field-Nigeria. Geosciences. 2012;2(3):60-65.
    DOI: 10.5923/j.geo.20120203.04
14. Aizebeokhai AP, Olayinka I. Structural and stratigraphic mapping of Emi field offshore Niger Delta. Journal of Geology and Mining Research. 2010;3(2):25-38.
15. Eshimokhai S. and Akhirevbulu OE. Reservoir characterization using Seismic and Well Logs Data (A case study of Niger Delta). Ethiopian Journal of Environmental Studies and Management. 2012;5:4.
16. Ajisafe YC, Ako BD. Seismic attributes for reservoir characterization of "Y" field Niger Delta, Nigeria. Journal of Applied Geology and Geophysics. 2013;1(2):23-31.
17. Journel AG. Geology and reservoir geology. Stochastic modeling and geostatistics. In: Yarus JM, Chambers RL (eds) AAPG Computer Applications in Geology, Tulsa, Oklahoma. 1995;3:19-20.
18. Whiteman A. Nigeria-its petroleum geology resources and potential: London, Graham and Trotman. 1982;394.

Available:http://www.rigzone.com/training/insight.asp?insight_id=301&c_id=1

19. Oyeyemi KD, Aizebeokhai AP. Seismic Attributes analysis for reservoir characterization; Offshore Niger Delta. Petroleum and Coal; 2015.
[ISSN 1337-7027]
Available:www.vurup.sk/petroleum-coal

20. Doust H, Omatsola E. Niger Delta, In, Edwards JD, Santogrossi PA, Eds., Divergent/Passive Margin Basins: Tulsa, American Association of Petroleum Geologists. 1990;48:239-248.

21. Salawu NB, Olatunji S, Orosun MM, Abdulraheem TY. Geophysical inversion of geologic structures of Oyo metropolis, southwestern Nigeria, from airborne magnetic data. Geomech. Geophys. Geo-energy Geo-resour; 2019.
Available:https://doi.org/10.1007/s40948-019-00110-7

22. Marsden DI. Layer cake depth conversion. Geophys Lead Edge. 1989;8:10–14.

Peer-review history:
The peer review history for this paper can be accessed here:
http://www.sdiarticle4.com/review-history/58527